

## Supporting Information

### Crystal-Phase Engineering of $\text{ZrS}_2/\gamma\text{-BC}_6\text{N}$ Heterostructures for Enhanced Type-II Photocatalytic Water Splitting

Peng Zhang,<sup>1</sup> Jiashuo Zhang,<sup>1</sup> Junhui Li<sup>1</sup> and Tongtong Li<sup>1\*</sup>

<sup>1</sup> China-Uzbekistan Joint Laboratory on Advanced Porous Materials, School of Materials Science and Engineering, Zhejiang Sci-Tech University, Hangzhou 310018, China.

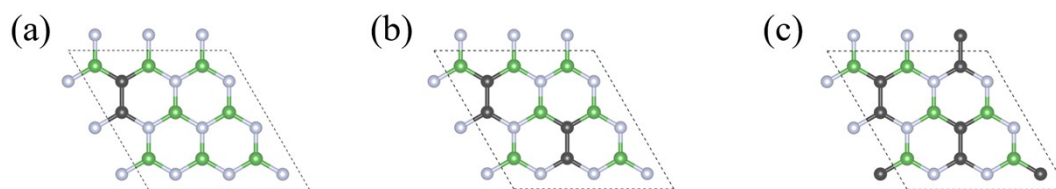


Fig.S1. (a-c) are top-down views of the single-layer structures  $\text{h-BC}_x\text{N}$  ( $x = 2, 4, 6$ ) respectively.

---

\*Corresponding Authors: Tongtong Li(yitaji@zstu.edu.cn)

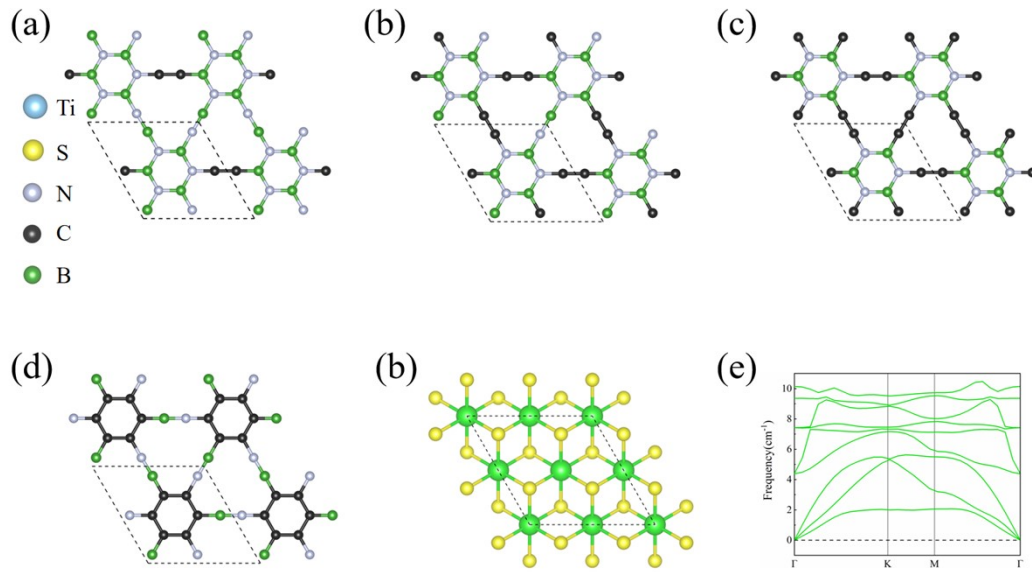


Fig.S2. (a–d) are top-down views of  $\gamma$ -BC<sub>x</sub>N monolayer structures ( $x = 2, 4, 6$ ), respectively. (e) and (f) are top-down views of the ZrS<sub>2</sub> monolayer structure and the corresponding high-symmetry  $K$ -path ( $\Gamma \rightarrow K \rightarrow M \rightarrow \Gamma$ ) phonon dispersion relations, respectively.

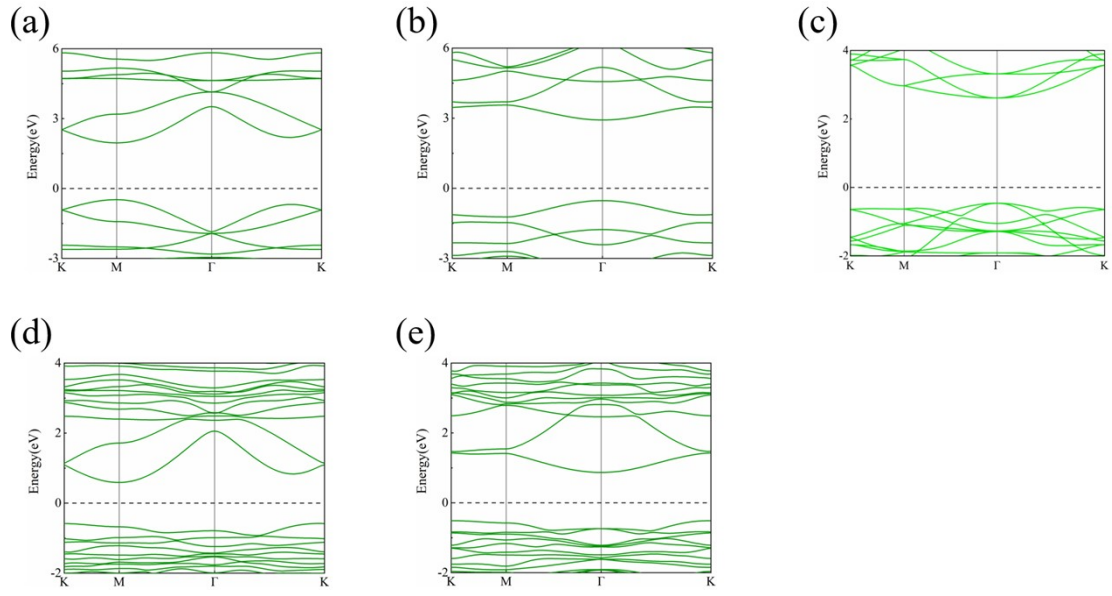


Fig.S3. (a-e) represent the band structures of  $\gamma$ -BC<sub>6</sub>N, h-BC<sub>4</sub>N, and monolayer ZrS<sub>2</sub>; and the heterostructures ZrS<sub>2</sub>/ $\gamma$ -BC<sub>6</sub>N and ZrS<sub>2</sub>/h-BC<sub>4</sub>N, respectively, as calculated by the PBE method.

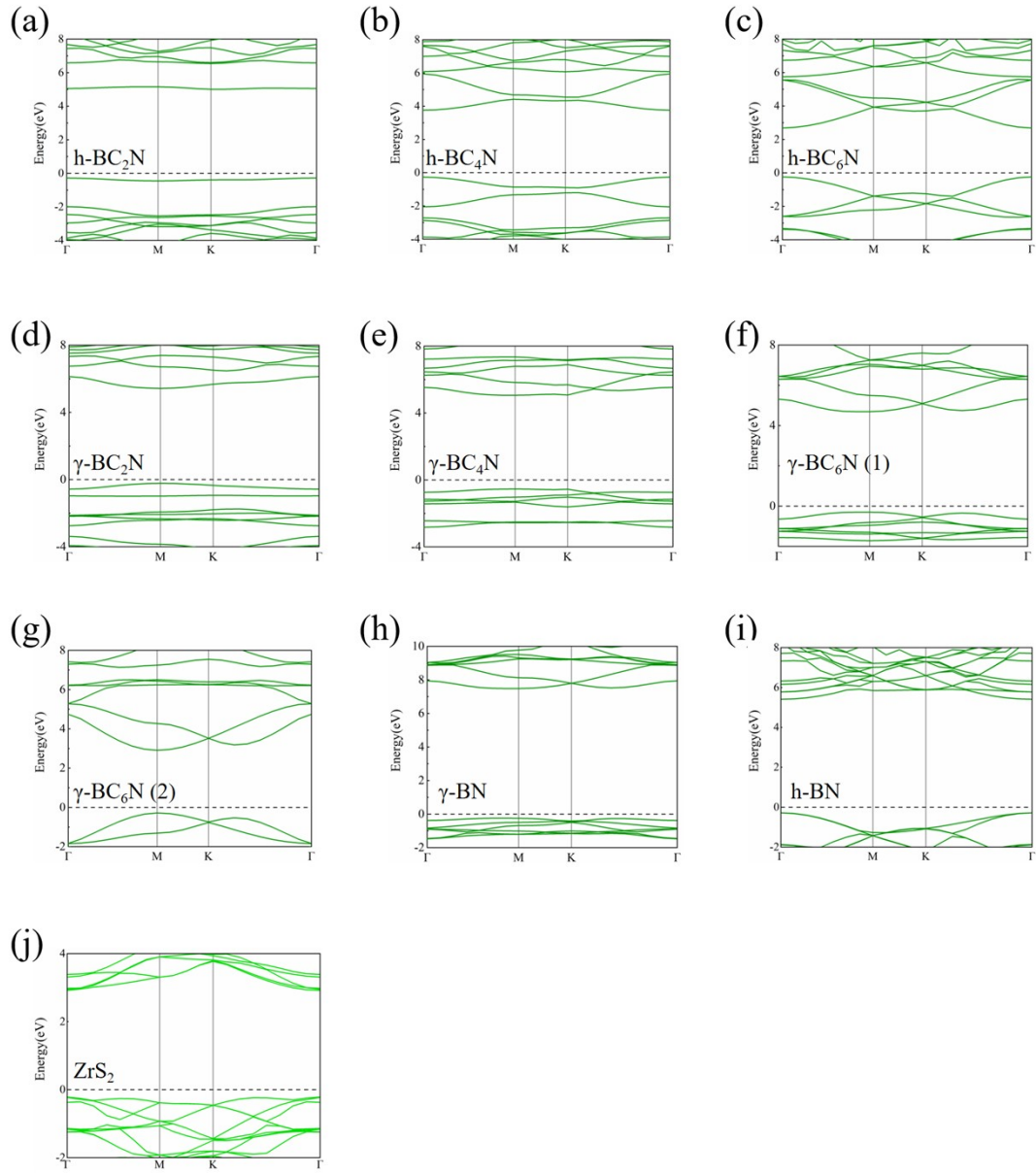


Fig.S4. (a-j) represent the band structure diagrams for each monolayer under the HSE06 method.

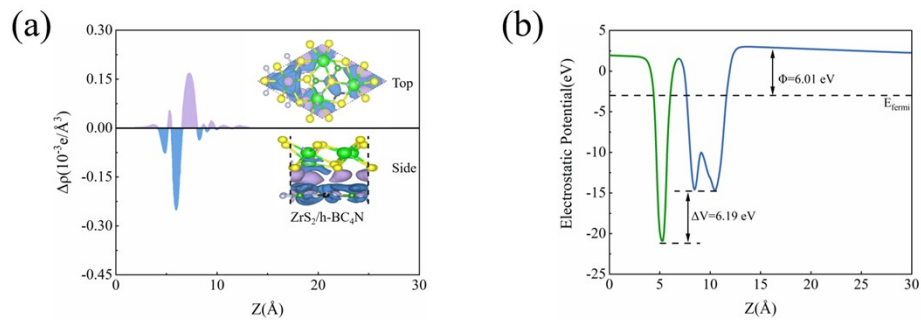


Fig.S5. (a) Charge density distribution map of the  $\text{ZrS}_2/\text{h-BC}_4\text{N}$  heterostructures (blue and purple in the inset denote charge accumulation and loss respectively). (b) Electrostatic potential distribution map of the  $\text{ZrS}_2/\text{h-BC}_4\text{N}$  heterostructures.

**Table S1.** The energy of CBM and VBM ( $E_{\text{CBM}}$  and  $E_{\text{VBM}}$ ), the overpotentials of HER and OER ( $\chi(\text{H}_2)$  and  $\chi(\text{O}_2)$ ), the calculated  $E_g$  ( $E_{\text{g-HSE06}}$ ) of HSE06, and the energy conversion efficiency  $\eta_{\text{STH}}$  of STH at the band-edge position of the different heterostructures under different strains

	Water splitting edges		$\chi(\text{H}_2)$ (eV)	$\chi(\text{O}_2)$ (eV)	$E_{\text{g-HSE06}}$ (eV)	$\eta_{\text{STH}}$ (%)
	$E_{\text{CBM}}$ (eV)	$E_{\text{VBM}}$ (eV)				
ZrS <sub>2</sub> / $\gamma$ -BC <sub>6</sub> N	-4.23	-5.64	1.62	0.33	2.3	15.54
ZrS <sub>2</sub> / $\gamma$ -BN	-3.92	-5.60	2.2	2.05	3.11	5.04
ZrS <sub>2</sub> /h-BC <sub>4</sub> N	-3.94	-5.69	0.71	0.86	3.06	5.8
ZrS <sub>2</sub> /h-BN	-4.08	-5.79	0.5	0.51	3.55	1.15

**Table S2.** Band gaps( $E_g$ ), CBO, power conversion efficiency (PCE) and absorption coefficient of different heterostructures.

	$E_g$	CBO	PCE	Absorption Coefficient
ZrS <sub>2</sub> / $\gamma$ -BC <sub>6</sub> N	2.3	0.2	10.5%	$4.10 \times 10^5 \text{ cm}^{-1}$
ZrS <sub>2</sub> / $\gamma$ -BN	3.06	0.33	4.78%	$1.80 \times 10^5 \text{ cm}^{-1}$
ZrS <sub>2</sub> /h-BC <sub>4</sub> N	3.55	0.3	2.45%	$2.80 \times 10^5 \text{ cm}^{-1}$
ZrS <sub>2</sub> /h-BN	2.77	0.27	10.37%	$1.73 \times 10^5 \text{ cm}^{-1}$

**Table S3.** Defect formation energy

	Energy(eV)
$\gamma$ -BC <sub>2</sub> N	-1.34250782
$\gamma$ -BC <sub>4</sub> N	-4.01080547
$\gamma$ -BC <sub>6</sub> N	-9.46246252